Advanced Pharmaceutical Bulletin

Accepted Manuscript (unedited)

The manuscript will undergo copyediting, typesetting, and review of the resulting proof before it is published in its final form.

Research Article

How to cite this article:
Karami K, Uroomiye SS, Derakhshandeh K, Nouri F, Chehardoli Gh, Haji Hosseini R. Development of Cationic Dextran Nanoparticles via Reductive Amination: Enhanced Cellular Uptake and Low Cytotoxicity in Gene Transfection. Advanced Pharmaceutical Bulletin, doi: 10.34172/apb.46469

Development of Cationic Dextran Nanoparticles via Reductive Amination: Enhanced Cellular Uptake and Low Cytotoxicity in Gene Transfection

Kianoosh Karami[1], Seyed Sepehr Uroomiye[2,3], Katayoun Derakhshandeh[2]*, Fatemeh Nouri[4], Gholamabbas Chehardoli[5], Reza Haji Hosseini[1]

[1] Department of Biology, Payame Noor University (PNU), Tehran, Iran
[2] Departmen of Pharmaceutics, School of Pharmacy, Medicinal Plants and Natural Products Research Center, Hamadan University of Medical Sciences, Hamadan, Iran
[3]Department of Tissue Engineering, School of Advanced Technologies in Medicine, Tehran University of Medical Sciences, Tehran, Iran
[4]Department of Pharmaceutical Biotechnology, School of Pharmacy, Hamadan University of Medical Sciences, Hamadan, Iran
[5] Department of Medicinal Chemistry, School of Pharmacy, Hamadan University of Medical Sciences, Hamadan, Iran

ARTICLE INFO

Keywords:
Gene Delivery,
Dextran,
Cationic Polymer,
Nanoparticles,
Non-viral Vector,
NIH3T3 Cells.

Article History:
Submitted: September 29, 2025
Revised: July 26, 2026
Accepted: August 14, 2026
ePublished: August 31, 2026

ABSTRACT

Purpose: The development of safe and efficient non-viral carriers remains critical for gene therapy. Biocompatible polysaccharides such as dextran are attractive candidates for novel delivery platforms. This study reports the synthesis, characterization, and evaluation of a cationic dextran derivative for pDNA delivery.
Methods: Cationic Dextran was synthesized through periodate oxidation and reductive amination with 1,6-Hexamethylenediamine. Its structure was confirmed using ^{1}H NMR and FT-IR spectroscopy. Nanoparticles, formed via self-assembly with pDNA, were analyzed for size, zeta potential (DLS), and morphology (SEM). Functional properties, including buffering capacity, pDNA condensation (gel retardation assay), DNase I protection, cytotoxicity in NIH3T3 cells (MTT assay), and cellular uptake, were assessed.
Results: Nanoparticles showed uniform size (207–245 nm) and strong positive zeta potential (+57.2 to +73.7 mV). The polymers demonstrated a substantial buffering capacity within the endosomal pH range, efficiently condensed pDNA, and provided partial protection against DNase I. Cytotoxicity was low at both 24 and 48 hours. Flow cytometry confirmed high cellular uptake, with over 95% of NIH3T3 cells internalizing polyplexes.
Conclusion: These cationic Dextran nanocarriers demonstrate efficient pDNA condensation, low cytotoxicity, and high cellular uptake, making them promising for gene delivery. Although nuclease protection needs optimization, it offers a versatile platform for non-viral gene therapy.

***Corresponding Author:**
Katayoun Derakhshandeh, Email: k.derakhshandeh@umsha.ac.ir, ORCID: 0000-0003-2650-244X

Introduction

Gene therapy represents a transformative approach in medicine, targeting the genetic basis of diseases to provide long-lasting or curative effects, unlike conventional treatments that primarily address symptoms.[1-3] This strategy involves delivering therapeutic nucleic acids, such as DNA or RNA, into target cells to restore or enhance gene function, offering potential for treating inherited disorders, cancers, and autoimmune diseases.[4-6] The success of gene therapy hinges on safe and efficient delivery systems, or vectors, to transport genetic material across biological barriers to intracellular targets.[7,8]

Gene transfer vectors can be divided into two major categories: viral and non-viral systems. Owing to their naturally evolved transduction pathways, viral vectors such as Adenoviruses, Retroviruses, and Adeno-Associated Viruses (AAVs) typically demonstrate high delivery efficiency.[9,10] However, concerns including immunogenicity, insertional mutagenesis, limited cargo capacity, and production challenges limit their clinical use.[11,12] These limitations have driven research into non-viral vectors, which are generally safer and more versatile.[13]

Non-viral vectors are typically synthetic or natural molecules engineered to mimic the function of Viruses in delivering nucleic acids. Polymers, as a versatile class of materials, exhibit a wide range of applications in various biomedical fields and have paved the way for enhancing theragnostic tools, such as drug delivery and gene delivery systems.[14] Due to their tunable features, such as ease of chemical functionalization, they have gained so much attention in the research fields of non-viral vectors.[15] Previous studies demonstrate the relation between some properties of a polymer, such as its charge density and molecular weight, and its success in the transfection process.[16] Among non-viral carriers, cationic polymers have attracted considerable attention because of their capacity to compact negatively charged nucleic acids into nanoscale complexes known as polyplexes. These structures not only shield DNA from enzymatic degradation by nucleases but also promote intracellular delivery through endocytic pathways.[17-19] In addition, efficient cationic polymers can facilitate endosomal release of the genetic cargo, frequently through a mechanism referred to as the "proton sponge effect".[20] Representative members of this class include Poly(L-lysine) (PLL), Polyethyleneimine (PEI), and Chitosan. Although PEI is commonly regarded as the benchmark polymer for transfection performance, its practical application is often constrained by its associated cytotoxicity[10,21,22]

To address these challenges, natural polymers like Dextran, a biocompatible and biodegradable polysaccharide composed of α-1,6-linked D-Glucopyranose units, have gained attention.[23-25] Dextran's hydroxyl groups allow chemical modification to introduce cationic moieties for DNA binding, and its FDA approval for clinical applications highlights its safety and low immunogenicity.[26,27]

Cationization strategies, such as grafting with PEI or spermine, have shown promise but may reintroduce cytotoxicity.[28,29] An alternative approach involves Periodate oxidation of Dextran's glucose units to form aldehyde groups, followed by reductive amination with a diamine to introduce primary amines, with the diamine linker influencing charge density, flexibility, and biodegradability.[30] Fibroblast cells, critical for connective tissue homeostasis through collagen and immunological mediator production, are implicated in autoimmune diseases and cancers when dysfunctional,[31-34] NIH3T3, a mouse embryonic fibroblast line, is used as a model for in vitro studies of fibroblasts, such as gene transfection studies.[35,36]

This study introduces a novel cationic Dextran derivative for gene delivery, synthesized via reductive amination of oxidized Dextran with 1,6-Hexamethylenediamine. We hypothesize that this modification yields a biocompatible polymer capable of condensing plasmid DNA into stable, nuclease-resistant nanoparticles with minimal toxicity. Three formulations with varying amination degrees were prepared to explore structure-activity relationships. The polymers and their polyplexes were characterized for physicochemical properties, including chemical structure, particle size, zeta potential, and morphology. Biological performance was evaluated through DNA condensation, protection, cytotoxicity, and cellular uptake in NIH3T3 cells. This work establishes a foundation for developing a safe, effective Dextran-based nanocarrier for gene therapy, with potential applications in treating malignancies and autoimmune diseases.

Materials and Methods

Materials

All chemicals employed in this study were of analytical and biological grade and were used as received unless otherwise specified. Dextran produced by *Leuconostoc mesenteroides* (average molecular weight: 9–11 kDa), sodium periodate, 1,6-hexamethylenediamine, sodium cyanoborohydride, ethylene glycol, dimethyl sulfoxide, sodium fluorescein, N,N′-dicyclohexylcarbodiimide, and 4-dimethylaminopyridine were supplied by Sigma-Aldrich (St. Louis, MO, USA). Cell culture reagents, including Dulbecco's Modified Eagle Medium, fetal bovine serum, penicillin–streptomycin solution, and trypsin–EDTA, were obtained from Gibco (Grand Island, NY, USA). The MTT reagent and SYBR Green I nucleic acid stain were purchased from Thermo Fisher Scientific (Waltham, MA, USA). NIH3T3 murine embryonic fibroblasts were provided by the National Cell Bank of the Pasteur Institute of Iran (Tehran, Iran). Double-deionized water was used throughout all experimental procedures requiring aqueous media.

Plasmid Properties

The plasmid used in this study was obtained from OriGene, which has the following specifications: The Cd200 (NM_010818) mouse tagged open reading frame (ORF) clone (catalog number MG203755) was obtained from OriGene Technologies. This expression plasmid encodes the full-length Cd200 ORF (834 bp; RefSeq NM_010818.3, NP_034948.3) fused to a TurboGFP tag, within the pCMV6-AC-GFP vector (PS100010). The clone is provided as 10 µg of ion-exchange purified, dried plasmid DNA, suitable for reconstitution in 100 µL of sterile water for transfection purposes.

Synthesis of Cationic Dextran

Oxidation of Dextran

Dextran was first oxidized to introduce aldehyde groups using a modified Malaprade reaction. Three separate reactions were set up to achieve different degrees of oxidation. For the preparation of oxidized dextran formulations, 0.5 g of dextran (approximately 0.05 mmol) was first dissolved in 10 mL of double-deionized water under continuous stirring. Subsequently, different quantities of sodium periodate were introduced into the reaction mixture to achieve distinct oxidation levels. Specifically, 0.25, 0.50, and 1.00 g of sodium periodate were used

for formulations F1, F2, and F3, respectively. The reaction mixtures were stirred in the dark at room temperature for 6 hours. The reaction was terminated by adding an excess of Ethylene Glycol to quench the unreacted Periodate. The resulting oxidized Dextran (Dextran-aldehyde) solution was purified by dialysis (MWCO 3,500 Da) against DDW for 48 hours, with the water being changed frequently. The purified product was then lyophilized to obtain a white powder.

Synthesis of Amine-Functionalized Dextran

The Dextran-aldehyde was subsequently cationized via reductive amination. 0.1 g of Dextran-aldehyde (from each of the three oxidation batches) was dissolved in 30 mL of water containing 3g of 1,6-Hexamethylenediamine. The mixture was stirred until the Dextran-aldehyde dissolved completely. Then, 1.5 g of Sodium cyanoborohydride ($NaBH_3CN$) was added as a reducing agent to form stable secondary amine linkages. Subsequently, the reaction mixture was incubated under room-temperature conditions for 24 h while being gently stirred throughout the process. The resulting cationic Dextran polymer (Dex-HD) was purified by extensive dialysis (MWCO 3,500 Da) against DDW for 48 hours to remove unreacted reagents and byproducts. The final product was obtained as a white, amorphous solid powder after lyophilization. The three formulations prepared from Dextran with low, medium, and high degrees of oxidation were designated as F1, F2, and F3, respectively.

Characterization of Cationic Dextran

Quantification of Aldehyde Groups

The aldehyde content in the oxidized Dextran was determined by a titration method using hydroxylamine hydrochloride. Briefly, a known amount of oxidized Dextran was dissolved in a hydroxylamine hydrochloride solution. The reaction between the aldehyde groups and hydroxylamine releases HCl. The amount of hydrochloric acid released during the reaction was determined by titration with a standardized 0.1 M sodium hydroxide solution while continuously monitoring the pH. Based on the titration results, the aldehyde content of the oxidized polymer was calculated. The oxidation degree was subsequently reported as the number of aldehyde functionalities corresponding to every 100 glucopyranose residues within the dextran structure.

Determination of Amine Content in Cationic Dextran

Lyophilized cationic dextran samples were weighed (10 mg) and dissolved in 1 mL DMSO (10 mg/mL). Aliquots (200 µL) were mixed with 800 µL ninhydrin reagent in 1.5 mL tubes. Tubes were centrifuged (10 s at 10,000 × g), incubated at 90°C for 45 min in a dry block thermostat, and cooled in an ice bath for 5 min. Reaction mixtures (500 µL) were transferred to 3 mL cuvettes, diluted with 2.5 mL 2-propanol/distilled water (50/50, v/v), and mixed. Absorbance was measured at 570 nm against blanks (200 µL DMSO + 800 µL reagent). Assays were performed in triplicate across three independent batches. Calibration was performed using glycine standards, and the resulting absorbance values recorded at 570 nm were plotted as a function of concentration (mM).

$$Amine\ content\ (mmol/g) = \frac{1}{{}_{sample}M} \times \frac{{}_{total}V}{{}_{aliquot}V} \times \frac{(A_{sample} - c)}{m}$$

$$DS(\%) = \left(\frac{Amine\ content\ \left(\frac{mmol}{g}\right) \times 162}{1000} \right) \times 100$$

The parameters used in the calculation are defined as follows: $M_{(sample)}$ represents the molecular weight of a single repeating unit expressed in g/mol; $V_{(total)}$ indicates the overall sample volume, while $V_{(aliquot)}$ refers to the portion withdrawn for analysis (mL). The term $A_{(sample)}$ corresponds to the experimentally determined absorbance. The constants *m* and *c* were obtained from the linear regression of the glycine calibration curve and denote its slope and intercept, respectively.

^{1}H NMR Spectroscopy

The chemical structures of the native Dextran, oxidized Dextran, and the final Dex-HD copolymer were verified through ^{1}H Nuclear Magnetic Resonance (^{1}H NMR) spectroscopy. The samples were dissolved in deuterated Dimethyl Sulfoxide (DMSO-d_6), and the spectra were recorded utilizing a Bruker Avance 400 MHz spectrometer (Bruker, Billerica, MA, USA).

FT-IR Spectroscopy

Fourier-transform infrared (FT-IR) spectroscopy was used to confirm the further functionalization of Dextran. The FT-IR spectra of native Dextran, oxidized Dextran, and Dex-HD were recorded on a Bruker Tensor 27 spectrometer in the range of 500–4000 cm^{-1} using KBr pellets.

Preparation and Characterization of Dex-HD/pDNA Polyplexes

Polyplexes were prepared by adding a specific amount of Dex-HD polymer (F2) solution to an equal volume of plasmid DNA (pDNA) solution at various N/P ratios. The N/P ratio is defined as the molar ratio of nitrogen atoms (N) in the cationic polymer to phosphate groups (P) in the pDNA. After preparation, the samples were gently homogenized using a vortex mixer and subsequently left at ambient temperature for 30 min, providing sufficient time for spontaneous complex assembly.

Determination of Hydrodynamic Diameter, Size Distribution, and Surface Potential

Particle size distribution and surface electrokinetic characteristics of the synthesized polyplexes were assessed with a Malvern Zetasizer Nano ZS system (Malvern Instruments, UK) based on Dynamic Light Scattering measurements. Data acquisition was performed at 25 °C and a 90° scattering geometry, and results were obtained from three independent measurements for each sample.

Scanning Electron Microscopy (SEM)

The morphology of the polyplexes was examined utilizing a Scanning Electron Microscope (TESCAN, Czech Republic). A drop of the polyplex solution was placed on a clean silicon wafer and air-dried. The sample was then sputter-coated with gold before imaging.

Buffering Capacity Assay

Buffering capacity was evaluated by potentiometric acid–base titration. Briefly, Dex-HD solutions (0.2 mg/mL, 30 mL in 150 mM NaCl) were adjusted to pH 10.0 using 0.1 N NaOH to ensure complete deprotonation of the amino groups. Subsequently, 0.1 N HCl was added stepwise under continuous stirring, and the pH was recorded after each addition until pH 5.0 was reached. A NaCl solution without polymer was analyzed under identical conditions as a control. The buffering behavior of the polymers was assessed from the resulting titration curves over the pH range relevant to endosomal acidification.

pDNA Condensation Assay (Gel Retardation)

DNA-binding and condensation properties of the Dex-HD polymers were assessed by monitoring plasmid migration in agarose gel electrophoresis. Complexes containing polymer and pDNA were formulated at predetermined N/P ratios and then applied to a 1.5% (w/v) agarose gel supplemented with SYBR Green I stain. The electrophoretic behavior of the samples was subsequently examined to evaluate complex formation. Agarose gel electrophoresis was conducted in TAE running buffer for 30 min at 90 V. DNA mobility was subsequently recorded under UV exposure using a gel documentation apparatus (Gel-Doc). Successful and complete pDNA condensation was evidenced by retention of the nucleic acid within the loading wells, with no observable electrophoretic migration.

DNase I Protection Assay

The protective effect of Dex-HD/pDNA complexes against nuclease-mediated degradation was investigated using a DNase I challenge assay. Polyplexes were first prepared at the selected N/P ratios and subsequently exposed to 10 µL of DNase I solution (1 U/µL) for 30 min at 37 °C. To stop the digestion process, 4 µL of 50 mM EDTA was added, after which the samples were heated at 65 °C for 10 min to ensure enzyme inactivation.

Following nuclease treatment, heparin was introduced to the samples, which were then maintained at room temperature for 30 min. This step promoted the disassembly of the polymer–DNA complexes and facilitated the release of entrapped plasmid DNA. Owing to its highly anionic nature, heparin competed with pDNA for interaction with the cationic Dex-HD chains, thereby disrupting the electrostatic association between the polymer and nucleic acid.

The recovered plasmid DNA was subsequently evaluated by electrophoresis on a 1.5% agarose gel containing SYBR Green I stain. DNase I-treated naked pDNA and untreated naked pDNA served as the negative and positive controls, respectively.

In Vitro Studies

Cell Culture

The NIH3T3 fibroblast cell line was propagated in complete DMEM containing 10% fetal bovine serum together with 100 U/mL penicillin and 100 µg/mL streptomycin. Throughout the study, cultures were kept in a temperature-controlled incubator at 37°C under humidified conditions with 5% CO_2.

Cytotoxicity Assay (MTT)

The cytotoxicity of the Dex-HD polymers and their polyplexes was evaluated using the MTT assay. NIH3T3 cells were seeded at a density of 5,000 cells/well in 96-well plates and incubated for 24 hours. The cells were then treated with various concentrations of the free Dex-HD polymers or Dex-HD/pDNA polyplexes. At predetermined time points (24, 48, and 72 h), the existing medium was carefully aspirated and substituted with 100 µL of fresh culture medium supplemented with 20 µL of MTT solution (5 mg/mL in PBS). Following a further 3 h incubation period, the insoluble formazan product formed by metabolically active cells was dissolved by adding 100 µL of DMSO to each well. Pursuing color development, absorbance readings were obtained at 570 nm using a microplate-based detection system. The viability of treated cells was determined by comparison with untreated controls and expressed as a percentage of the corresponding control response.

Fluorescein Labeling of Dextran

For cellular uptake studies, Dex-HD was labeled with Fluorescein. Fluorescein labeling of Dex-HD was achieved through coupling of the activated carboxyl functionality of Fluorescein with the available amino groups on the polymer backbone using Steglich-type reaction conditions. Briefly, 5 mg of Dex-HD, together with 62 mg of DCC and 37 mg of DMAP, was dissolved in 10 mL of DMSO. Subsequently, 100 mg of Fluorescein Sodium salt was introduced into the reaction mixture under continuous stirring. An inert nitrogen atmosphere was maintained throughout the 24 h reaction period. Thereafter, purification of the synthesized Dex-HD-FC conjugate was achieved by extensive dialysis against double-deionized water to remove residual low-molecular-weight components.

Qualitative Cellular Uptake

Fluorescence microscopy was employed to visualize the cellular uptake of the polyplexes. NIH3T3 cells were seeded on glass coverslips in a 6-well plate at a density of 150,000 cells/well. After 24 hours, the cells were treated with polyplexes formed between Dex-HD-FC and pDNA. Cells treated with free Dex-HD-FC served as a control. Following a 24-hour incubation period, the cells underwent three washes with PBS. The cellular uptake was examined under a fluorescence microscope (Olympus, Japan) utilizing an excitation wavelength of 490 nm.

Quantitative Transgene Expression Analysis

For gene delivery experiments, NIH3T3 cells were cultured in 6-well plates until approximately 70–80% confluence was achieved. The growth medium was then removed and replaced with 1500 µL of serum-free DMEM containing polyplex formulations corresponding to 2 µg of plasmid DNA per well. Cells were exposed to the polyplexes for 4 h at 37°C under a humidified atmosphere supplemented with 5% CO_2. Following the incubation period, the transfection medium was discarded and substituted with complete DMEM supplemented with 10% FBS. The cells were subsequently maintained for an additional 48 h to permit turboGFP expression.

Untreated cells and cells exposed to naked plasmid DNA (5 µg/well) in the absence of cationic dextran served as negative controls. Each experimental condition was evaluated in triplicate.

The transfection performance of the formulations was quantified by flow cytometric analysis of turboGFP expression. At 48 h after transfection, cells were rinsed twice with phosphate-buffered saline (PBS, pH 7.4) and harvested using 0.25% trypsin-EDTA. The collected cells were resuspended in PBS supplemented with 2% FBS and 1 mM EDTA to minimize cell aggregation prior to analysis. Measurements were carried out using a BD FACSCalibur flow cytometer equipped with a 482 nm argon-ion laser. Detection of turboGFP fluorescence was performed through the FL1 channel using a 530/30 nm band-pass filter. For each sample, at least 10,000 cellular events were recorded. Data processing was conducted using FlowJo software (version 10.8.1, BD Biosciences). Cellular debris and doublets were excluded through sequential gating based on forward scatter (FSC) and side scatter (SSC) characteristics. Transfection efficiency was calculated as the proportion of GFP-expressing cells relative to the untreated control population, while the mean fluorescence intensity (MFI) of GFP-positive cells was used as an indicator of transgene expression level.
Results are reported as mean ± standard deviation (SD) obtained from three independent experiments. Statistical comparisons among groups were performed using one-way analysis of variance (ANOVA) followed by Tukey's post hoc multiple-comparison test in GraphPad Prism (version 9.0; GraphPad Software, San Diego, CA, USA). Differences were considered statistically significant when p-values were less than 0.05.

Statistical Analysis

Quantitative measurements obtained from at least three separate experiments were summarized as mean ± SD. Statistical evaluation of group differences was performed through one-way ANOVA, with subsequent post hoc assessment using Tukey's correction for multiple comparisons. A significance criterion of $p < 0.05$ was adopted for all statistical analyses.

Results and Discussion

Synthesis and Characterization of Cationic Dextran

Cationic Dextran (Dex-HD) was synthesized in a two-step process involving Periodate oxidation and subsequent reductive amination with 1,6-hexamethylenediamine. The degree of oxidation, and consequently the degree of amine substitution, was controlled by varying the concentration of Sodium Periodate. The aldehyde content in the three oxidized Dextran batches was quantified by titration. The results showed a direct correlation between the amount of Periodate used and the resulting aldehyde content. For the batches prepared with 0.25 g, 0.5 g, and 1 g of Periodate, the aldehyde contents were 22.2%, 53.5%, and 64.6% (% w/w), respectively (Table 1). These different degrees of functionalization were expected to influence the physicochemical and biological properties of the resulting cationic polymers.

Table 1. Aldehyde content of oxidized Dextran as a function of Sodium Periodate used in the reaction.

Corresponding Formulation	Aldehyde Content (% w/w)	Sodium Periodate (g)
F1	22.2 ± 2.1	0.25
F2	53.5 ± 3.4	0.5
F3	64.6 ± 4.5	1.0

The chemical composition of the synthesized Dex-HD copolymer was assessed by ^{1}H NMR and FT-IR techniques. Characteristic resonances and absorption bands observed in the corresponding spectra provided evidence for the successful incorporation of the desired functional groups into the polymer structure. New signals emerged in the range of 1.2-1.8 ppm, corresponding to the methylene protons of the Hexamethylenediamine moiety grafted onto the Dextran backbone. The conjugation was further supported by the presence of a broad signal around 8.6-9.0 ppm, which could be attributed to the amine/imine protons (Figure 1, A and B).

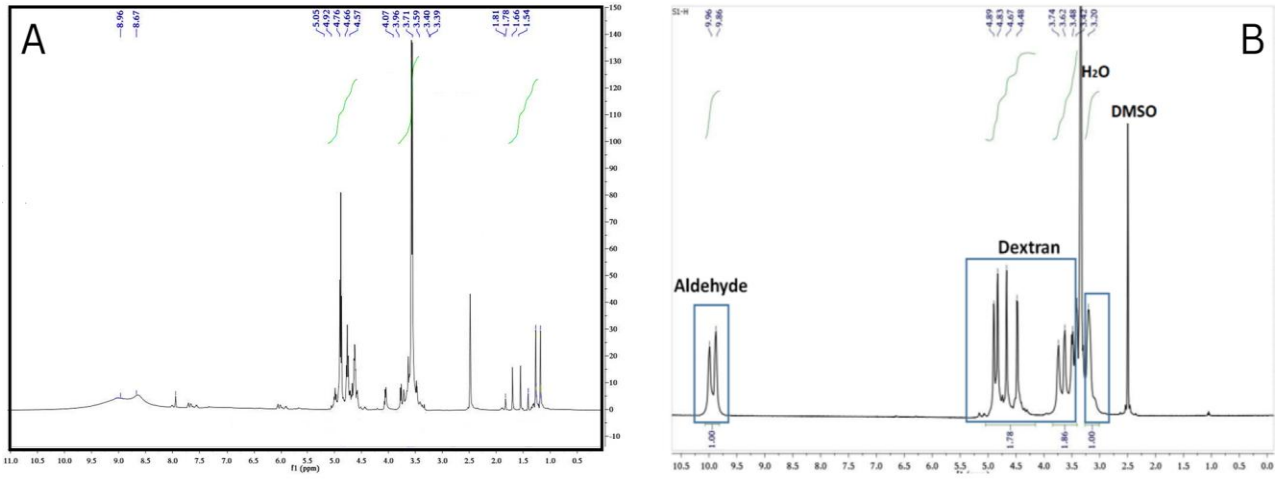

Figure 1. ^{1}HNMR spectra of **A)** dextran-1,6-hexanediamine copolymer dissolved in DMSO, **B)** Oxidized dextran (dextran aldehyde)

The FT-IR spectra (Figure 2) provided further evidence of the successful synthesis. The spectrum of oxidized Dextran showed a new characteristic absorption band at around 1730 cm^{-1}, corresponding to the C=O stretching vibration of the aldehyde groups. In the spectrum of the Dex-HD copolymer, this aldehyde peak was significantly diminished, while new peaks appeared. Specifically, the peak around 1548 cm^{-1} can be assigned to the N-H bending vibration of the secondary amines formed. The broadband around 3400 cm^{-1} (O-H and N-H stretching) was present in all spectra.

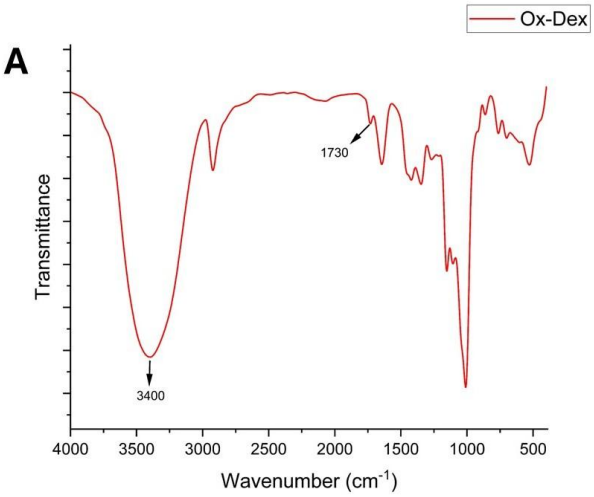

Figure 2 - A

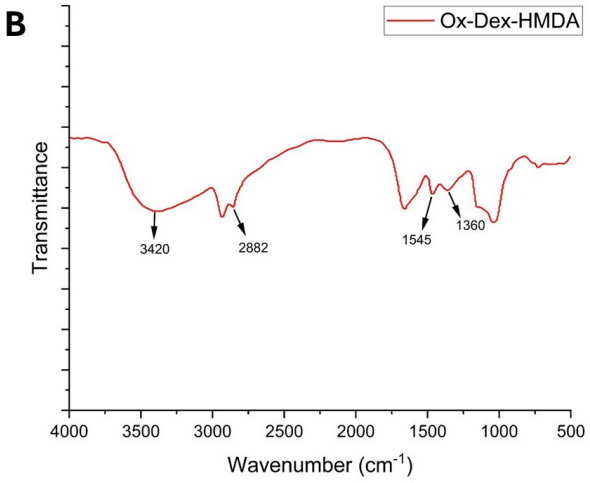

Figure 2 – B

Figure 2. FT-IR spectra of **A)** Oxidized Dextran (Dextran Aldehyde) and the final **B)** Dex-HD copolymer, confirming the chemical modifications.

Physicochemical Characterization of Dex-HD/pDNA Polyplexes

The Dex-HD polymers were able to condense pDNA into nanoparticles through electrostatic interactions. The size, PDI, and zeta potential of the polyplexes formed from the three Dex-HD formulations were measured by DLS (Table 2). All three formulations formed nanoparticles in the nanometer range. F2 formed the smallest particles with an average size of 207 nm and the lowest PDI of 0.181, indicating a relatively narrow size distribution. Formulations F1 and F3 formed slightly larger particles (230 nm and 245 nm, respectively). All polyplexes exhibited a strong positive surface charge, with zeta potentials ranging from +57.2 mV to +73.7 mV. The positive charge increased with the degree of amination (F1 < F2 < F3), which is crucial for interacting with the negatively charged cell membrane and facilitating cellular uptake.

Table 2. Physicochemical properties of Dex-HD/pDNA polyplexes.

Formulation	Particle Size (nm)	PDI	Zeta Potential (mV)
F1	230 ± 15	0.220 ± 0.04	+57.2 ± 3.1
F2	207 ± 11	0.181 ± 0.03	+65.4 ± 2.8
F3	245 ± 18	0.252 ± 0.07	+73.7 ± 4.2

Degree of substitution for prepared Formulation

The result of the Ninhydrin assay revealed that the highest 1,6-hexanediamine degree of substitution in the different prepared Dex-HD polymers is for F3, followed by F2 and F1, respectively. Properties of various polyplexes, prepared using different N/P ratios, are presented in Table 3.

Table 3. N/P ratio for F1, F2, and F3 polyplexes formed using cationic Dextran with a 23%, 30%, and 45% degree of substitution.

Degree of Substitution	Plate Type	DNA Amount	N/P Ratio	Phosphate (nmol)	Nitrogen (nmol)	Cationic Dextran (µg)	Volume at 1 mg/mL (µL)
23%	6-Well	10 µg	2:1	30.8	61.6	50.18	50.18
23%	6-Well	10 µg	5:1	30.8	154	125.46	125.46
30%	6-Well	10 µg	2:1	30.8	61.6	38.58	38.58
30%	6-Well	10 µg	5:1	30.8	154	96.45	96.45
45%	6-Well	10 µg	2:1	30.8	61.6	28.11	28.11
45%	6-Well	10 µg	5:1	30.8	154	70.27	70.27

SEM Image Analysis of Polyplex

The morphology of the polyplexes was observed by SEM. The images revealed that the polyplexes were predominantly spherical and had a relatively uniform size distribution, consistent with the DLS results. The particles appeared to be well-dispersed with minimal aggregation (The buffering capacity was added to the supplementary file).

Buffering Capacity

The buffering behavior of the Dex-HD formulations was characterized by acid-base titration across the pH range relevant to endosomal maturation. The control solution (H_2O/NaCl) underwent a sharp pH decline upon HCl addition, while all Dex-HD formulations displayed markedly greater resistance to acidification, reflecting the presence of protonable amino groups within the polymer architecture.

Of the three formulations, F3 showed the strongest buffering capacity, with F2 and F1 following in decreasing order. The superior performance of F3 is likely due to its higher degree of amine substitution, which supplies a

larger number of proton-accepting sites. Importantly, every formulation retained buffering activity over the pH window of roughly 5.0–7.0, the range encountered during endosomal acidification.

The buffering capacity trend (F3 > F2 > F1) aligns with the increasing degree of amination quantified by the ninhydrin assay, further supporting the successful chemical modification of dextran (The buffering capacity was added to the supplementary file).

pDNA Condensation and Protection

The ability of the Dex-HD polymers to condense pDNA was evaluated by a gel retardation assay (Figure 3). Naked pDNA migrated through the agarose gel, while pDNA complexed with the cationic polymers showed retarded migration. All three formulations were able to fully condense the pDNA, as indicated by the retention of the DNA in the loading wells. Complete condensation was observed at different N/P ratios (2:1 – 5:1) for the various formulations, correlating with their amine content. This confirms that the electrostatic interaction between the cationic polymer and pDNA is the driving force for condensation.

Protection of the incorporated plasmid DNA against DNase I-induced degradation was examined by exposing the polyplex formulations to nuclease treatment and evaluating the stability of the associated genetic material (Figure 3). Naked pDNA was completely degraded after incubation with DNase I (Lane 10). In contrast, the pDNA in the polyplexes was partially protected from nuclease digestion. F3 (Lane 9) provided the best protection, with a visible band of intact pDNA remaining after treatment. F1 (Lane 7) and F2 (Lane 8) also provided some protection, albeit to a lesser extent. This suggests that the compact structure of the polyplexes shields the pDNA from nuclease access, although the protection is not absolute.

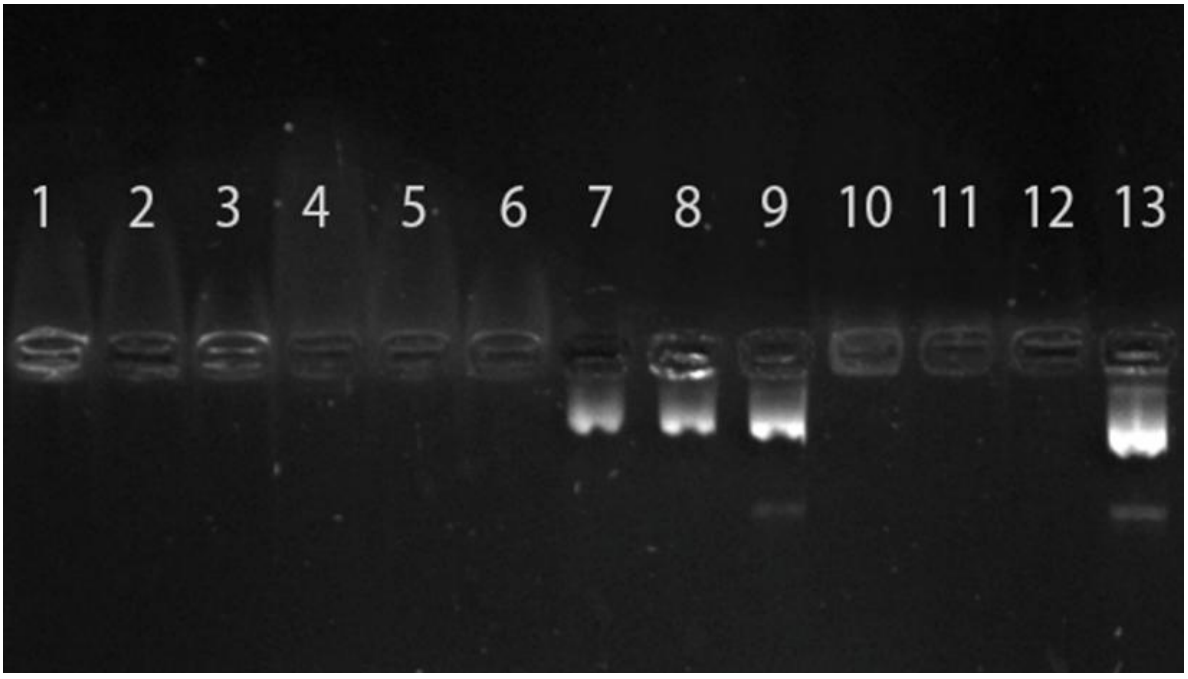

Figure 3. Effects of Different Formulations on the Condensation Process and Protection Against DNase I Degradation. **(A)** Lane 1 and 2: Polyplex prepared with F1 (N/P 2:1 and 5:1 respectively), **(B)** Lane 3 and 4: Polyplex prepared with F2 (N/P 2:1 and 5:1 respectively), **(C)** Lane 5 and 6: Polyplex prepared with F3 (N/P 2:1 and 5:1 respectively), **(D)** Lane 7, 8, and 9: Plasmids complexed with F1, F2, and F3, respectively, and subjected to DNase I treatment (N/P 5:1), **(E)** Lane 10: Naked plasmid exposed to DNase I enzyme, **(F)** Lane 11: Replicate of naked plasmid exposed to DNase I enzyme, **(G)** Lane 12: Equal amount of different free copolymer in the presence of DNase I enzyme, **(H)** Lane 13: Free naked plasmid (control, without DNase I treatment)

Cytotoxicity Assessment

The cytotoxicity of the Dex-HD polymers and their polyplexes were evaluated in NIH3T3 cells using the MTT assay over 72 hours (Figure 4). At 24 and 48 hours, all three free polymer formulations (F1, F2, F3) exhibited high cell viability (>80%) even at the highest concentrations tested, indicating low short-term toxicity. However, after 72 hours of incubation, the F3 formulation, which has the highest charge density, showed a concentration-dependent decrease in cell viability. The polyplexes generally exhibited slightly higher toxicity than the free polymers; however, overall, cell viability remained high, especially for F1 and F2. The results, presented in Figure 4-G, demonstrate that PEI exhibits significant dose- and time-dependent cytotoxicity. Across all time points, an increase in PEI concentration led to a corresponding decrease in cell viability. Cell viability remained above 90% after 24 hours at the lowest concentration tested (39.060 µg/mL), but it dropped to about 70% after 72 hours, suggesting a time-dependent effect. This cytotoxic effect was more pronounced at higher concentrations. For instance, at 312.500 µg/mL, cell viability was reduced to approximately 70%, 62%, and 44% after 24, 48, and 72 hours, respectively (Table 4).

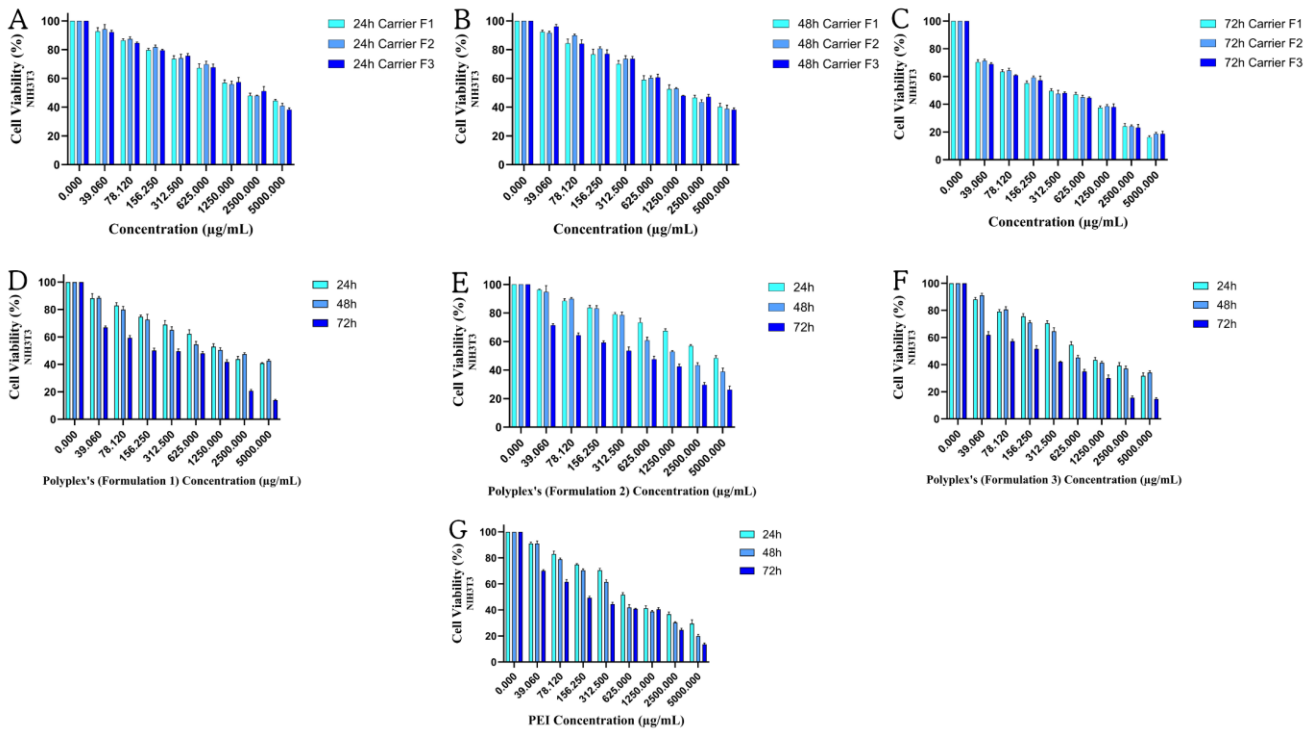

Figure 4. Cell viability of NIH3T3 cells treated with different concentrations of Dex-HD polymers (**A**: 24h, **B**: 48h, **C**: 72h),(**D**) F1 polyplexes, (**E**) F2 polyplexes, (**F**) F3 polyplexes, (**G**) PEI as determined by the MTT assay. Data are mean ± SD (n=3).

Table 4. The Average IC_{50} of different investigated compounds over the study time.

	Average IC_{50} 24h (µg/ml)	Average IC_{50} 48h (µg/ml)	Average IC_{50} 72h (µg/ml)
F1	1829	1698	445.4
F2	1810	1426	334.0
F3	1374	1017	266.6
PEI	857.9	560.4	251.1
Polyplex F1	1495	1315	334.8
Polyplex F2	2880	1517	431.4
Polyplex F3	1092	852.7	215.3

Cellular Uptake

The extent of polyplex internalization by NIH3T3 cells was examined using both fluorescence microscopy and flow cytometry, providing qualitative and quantitative information, respectively. To facilitate monitoring of cellular uptake, the Dex-HD carrier was labeled with Fluorescein (FC). As shown in Figure 5, cells treated with FC-labeled polyplexes displayed strong green fluorescence in the cytoplasm, indicating successful internalization of the nanoparticles. In contrast, cells treated with free FC-labeled Dextran showed only faint, diffuse fluorescence, confirming that the nanoparticle formulation is essential for efficient uptake.

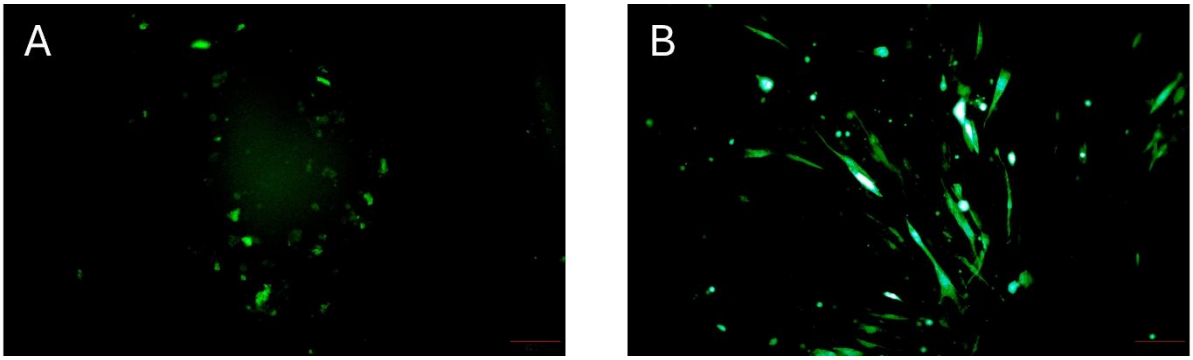

Figure 5. Fluorescence microscopy images of NIH3T3 cells after 24h incubation with (**A**) control cells, and (**B**) FC-labeled Dex-HD/pDNA polyplexes. The bright green fluorescence in (B) indicates efficient cellular uptake.

The quantitative analysis of cellular transfection efficiency, as determined by flow cytometry, further confirmed these observations (Figure 6). Analysis of the Green Fluorescent Protein gene as a reporter is used to evaluate the gene transfection process. Cells exposed to polyplexes derived from all three formulations demonstrated a substantial augmentation in fluorescence intensity relative to control cells and those treated with free pDNA. The percentage of fluorescently positive cells was remarkably high: 95.3% for F1, 95.5% for F2, and 97.1% for F3. This indicates that the vast majority of the cells had taken up the pDNA-loaded nanoparticles.

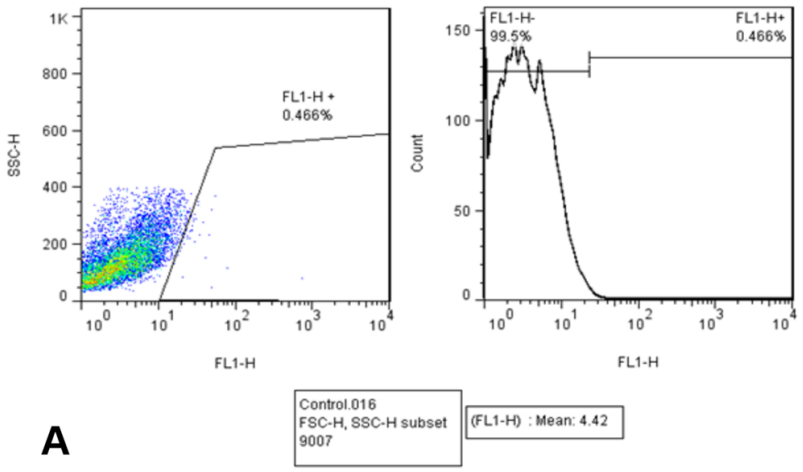
SSC-H
FL1-H
FL1-H +
0.466%
Count
FL1-H-
99.5%
FL1-H+
0.466%
Control.016
FSC-H, SSC-H subset
9007
(FL1-H) : Mean: 4.42

A

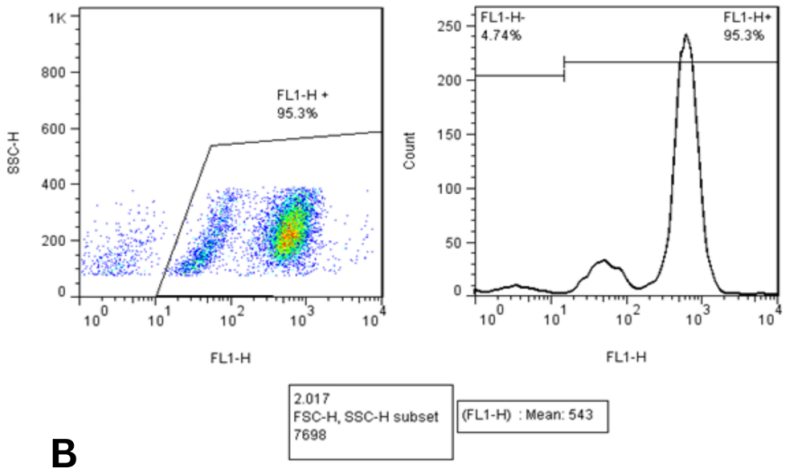
SSC-H
FL1-H
FL1-H +
95.3%
Count
FL1-H-
4.74%
FL1-H+
95.3%
2.017
FSC-H, SSC-H subset
7698
(FL1-H) : Mean: 543

B

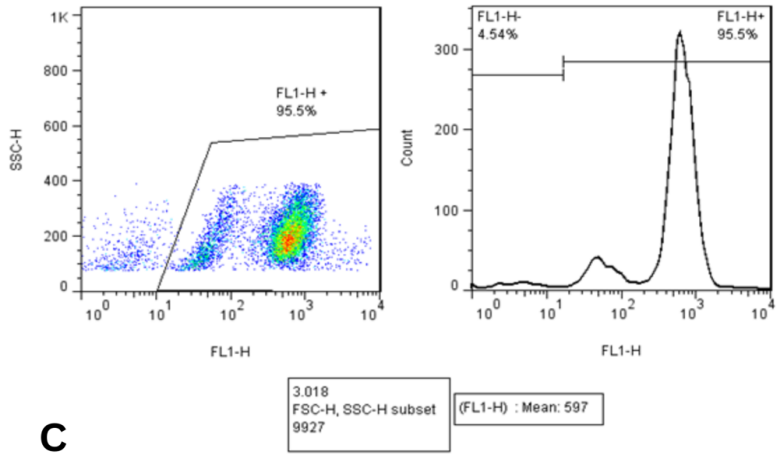
SSC-H
FL1-H
FL1-H +
95.5%
Count
FL1-H-
4.54%
FL1-H+
95.5%
3.018
FSC-H, SSC-H subset
9927
(FL1-H) : Mean: 597

C

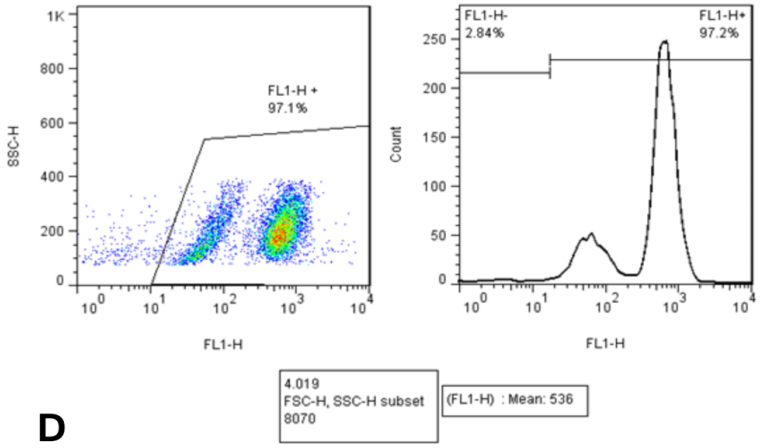

Figure 6. Fluorescent analysis of Green Fluorescent Protein using flow cytometry of pDNA in NIH3T3 cells. Histograms show (**A**) control (Untreated cells), (**B**) cells treated with polyplex F1, (**C**) cells treated with polyplex F2, and (**D**) cells treated with polyplex F3. The high percentage of fluorescent cells in B, C, and D confirms efficient uptake.

The overarching goal of this research was to develop a safe and effective non-viral gene delivery system based on the natural polysaccharide Dextran. Our study's findings provide a thorough assessment of the potential of a number of cationic Dextran-graft-hexamethylenediamine (Dex-HD) polymers as gene carriers by demonstrating their successful synthesis. The key findings highlight the promising characteristics of these novel vectors, including their ability to form stable nanoparticles with pDNA, their low cytotoxicity, and their efficiency in mediating cellular uptake.

The synthesis strategy employed, involving Periodate oxidation followed by reductive amination, proved to be an effective method for introducing cationic charge to the Dextran backbone. The ^{1}H NMR and FT-IR analyses conclusively confirmed the chemical transformations, showing the appearance of aldehyde groups after oxidation and their subsequent conversion to secondary amine linkages upon reaction with 1,6-hexamethylenediamine. By controlling the initial degree of oxidation, we were able to create three formulations (F1, F2, F3) with varying densities of amine and aldehyde groups. This control over the chemical structure is crucial, as the charge density of a cationic polymer is a primary determinant of its interaction with nucleic acids and cells.[37]

The capacity of cationic carriers to compact nucleic acids into nanosized assemblies is a key determinant of successful gene transfer. Analysis by DLS together with SEM imaging confirmed the spontaneous formation of uniform Dex-HD/pDNA complexes for all formulations, yielding spherical particles with average diameters in the 200–250 nm range. From a biological perspective, nanoparticles of this dimension are particularly favorable because they can efficiently enter cells through endocytic mechanisms while avoiding the rapid clearance typically associated with substantially smaller particles.[38] Notably, the F2 formulation, with an intermediate degree of amination, yielded the smallest and most monodisperse particles, suggesting that an optimal balance between hydrophilic and cationic forces may promote more efficient and uniform self-assembly. The polyplexes exhibited a strong positive zeta potential, which is essential for initiating electrostatic interactions with the negatively

charged proteoglycans on the cell surface, the first step in cellular entry.[39] As expected, the zeta potential increased with the degree of amination, with F3 showing the highest surface charge.

The gel retardation assay further confirmed the strong DNA-binding capacity of the Dex-HD polymers. The complete condensation of pDNA, indicated by its retention in the gel wells, underscores the strength of the electrostatic interactions. The fact that F3, the polymer with the highest amine content, required the lowest N/P ratio for complete condensation follows the expected structure-activity relationship: a higher charge density leads to more efficient neutralization of the DNA's negative charge.[40] This efficient condensation is also critical for protecting the genetic cargo from degradation. The DNase I protection assay showed that the polyplexes, particularly those formed with F3, offered significant protection against nuclease attack compared to naked pDNA. While the protection was not absolute, it suggests that the compact structure of the polyplexes effectively shields the DNA from damage. Incomplete protection is a common challenge for non-viral vectors, indicating that polyplexes may have a dynamic structure, with some regions of the DNA occasionally becoming accessible.[41] Further optimization, such as cross-linking the polyplexes, could potentially enhance their stability and nuclease resistance for in vivo applications.

A significant advantage of using natural polymers such as Dextran is the potential for improved biocompatibility compared to synthetic polymers like PEI. Our cytotoxicity studies using the MTT assay largely supported this premise. At 24 and 48 hours, all Dex-HD formulations demonstrated low cytotoxicity in NIH3T3 cells, even at high concentrations. This represents a significant improvement over PEI, which is known to cause considerable cytotoxicity due to its high and non-degradable charge density.[42] The delayed toxicity observed with the F3 formulation after 72 hours is likely attributable to its higher charge density, which can lead to cumulative stress on the cells over time.[43] Overall, the Dex-HD carriers, especially F1 and F2, demonstrated an acceptable safety profile.

The cellular interaction profile of the Dex-HD/pDNA complexes revealed efficient intracellular accumulation within NIH3T3 cells. Qualitative observations from fluorescence imaging, together with quantitative flow cytometry data, consistently indicated that more than 95% of the treated cells were associated with detectable fluorescence signals. Another important property identified for the Dex-HD carrier was its buffering capability, confirmed through acid–base titration analysis, which is considered a key feature influencing intracellular trafficking and subsequent gene delivery performance. It is hypothesized that the protonation of the polymer's amine groups in the acidic environment of the endosome facilitates the "proton sponge" effect, thereby inducing an influx of ions and water, which results in endosomal swelling rupture.[44] This proposed mechanism is critical for the escape of the polyplex from the endo-lysosomal pathway, a significant barrier to successful gene delivery.

However, appraising the Green Fluorescent Protein, fluorescence emission using flow cytometry indicates the successful reporter gene expression, which can be interpreted as a sign of this system's compatibility with the NIH3T3 gene expression system. Cellular internalization represents only one component of the gene delivery pathway. Following uptake, the transported nucleic acid must successfully overcome multiple intracellular barriers, including endosomal sequestration, transit through the cytoplasmic environment, and access to the nuclear compartment, each of which can affect the final level of gene expression.[45] To advance this platform

toward the specific therapeutic goals outlined in the introduction, subsequent work must also evaluate its efficacy in delivering the therapeutic genes in cell lines relevant to cancer and immunological cell lines.

Conclusion

In summary, this study successfully designed, synthesized, and characterized a novel non-viral gene delivery system based on cationic Dextran. The Dextran-graft-hexamethylenediamine (Dex-HD) polymers have been demonstrated to effectively condense plasmid DNA into stable, positively charged nanoparticles of an appropriate size for cellular internalization. These nanoparticles demonstrated excellent biocompatibility and low cytotoxicity, particularly at shorter incubation times, and exhibited a remarkable ability to be internalized by NIH3T3 cells. Although additional optimization is necessary to enhance nuclease protection, the convergence of advantageous physicochemical attributes and elevated biological efficacy renders this Dextran-based nanocarrier a promising platform, thereby justifying further exploration for prospective gene therapy applications. Overall, the present study advances the ongoing development of polymer-based non-viral gene carriers and demonstrates the potential of Dex-HD as a clinically attractive platform that may overcome some of the safety limitations associated with viral delivery approaches while maintaining applicability to multiple disease targets.

Ethical Approval

This study was conducted with permission from the Ethics Committee of Hamadan University of Medical Sciences with code IR.UMSHA.REC.1403.283.

Authors' Contribution

Conceptualization: Kianoosh Karami, Katayoun Derakhshandeh, Seyed Sepehr Uroomiye
Data curation: Kianoosh Karami, Seyed Sepehr Uroomiye
Formal analysis: Katayoun Derakhshandeh, Kianoosh Karami, Seyed Sepehr Uroomiye
Investigation: Kianoosh Karami, Seyed Sepehr Uroomiye
Methodology: Gholamabbas Chehardoli, Kianoosh Karami, Seyed Sepehr Uroomiye
Project administration: Katayoun Derakhshandeh
Resources: Katayoun Derakhshandeh
Software: Kianoosh Karami
Supervision: Fatemeh Nouri, Katayoun Derakhshandeh
Validation: Seyed Sepehr Uroomiye, Katayoun Derakhshandeh
Writing–original draft: Kianoosh Karami
Writing–review & editing: Katayoun Derakhshandeh, Fatemeh Nouri, Seyed Sepehr Uroomiye, Gholamabbas Chehardoli, Reza Haji Hosseini

Acknowledgements

The authors would like to acknowledge the financial support provided by the Vice Chancellor for Research & Technology, Hamadan University of Medical Sciences.

Declaration of the Use of Artificial Intelligence in Manuscript Preparation

The authors used Gemini AI (version 2.5 Pro) as a linguistic editing aid during manuscript preparation. Its contribution was limited to improving language quality, enhancing readability, and correcting spelling and grammatical inconsistencies. No scientific content, data interpretation, experimental design, or conclusions were generated by the AI system. All modifications introduced through AI-assisted editing were critically evaluated and, where appropriate, further revised by the authors. The authors retain complete responsibility for the content and final published form of this work.

References

1. Pathak S. Gene therapy–Principles and applications. *Glob J Transfus Med* 2022;7(1):3-6. doi:10.4103/gjtm.gjtm_87_21

2. Jafarlou M, Baradaran B, Saedi T, Jafarlou V, Shanehbandi D, Maralani M, et al. An overview of the history, applications, advantages, disadvantages and prospects of gene therapy. *J Biol Regul Homeost Agents* 2016;30(2):315-21. PMID: 27358116

3. Patel MP. Gene Therapy for Cancer Treatment: Recent Trends and Clinical Evidence. In: Gene Delivery Systems. London: Taylor & Francis Group (CRC Press); 2022. P. 18.

4. Allen R, Yokota T. Endosomal Escape and Nuclear Localization: Critical Barriers for Therapeutic Nucleic Acids. *Molecules* 2024;29(24):5997. doi:10.3390/molecules29245997

5. Shu S-A, Wang J, Tao M-H, Leung PS. Gene therapy for autoimmune disease. *Clin Rev Allergy Immunol* 2015;49(2):163-76. doi:10.1007/s12016-014-8451-x

6. Islam MA, Kundu S, Hassan R. Gene therapy approaches in an autoimmune demyelinating disease: multiple sclerosis. *Curr Gene Ther* 2019;19(6):376-85. doi:10.2174/1566523220666200306092556

7. Arjmand B, Larijani B, Sheikh Hosseini M, Payab M, Gilany K, Goodarzi P, et al. The horizon of gene therapy in modern medicine: advances and challenges. *Cell Biology and Translational Medicine, Volume 8: Stem Cells in Regenerative Medicine* 2019:33-64. doi:10.1007/5584_2019_463.

8. Marguillier L, Dubruel P, Van Vlierberghe S. Gene Therapy Approaches Toward Biomedical Breakthroughs. Polymer and Photonic Materials Towards Biomedical Breakthroughs: Springer; 2018. p. 153-76. doi:10.1007/978-3-319-75801-5_6.

9. Tsai A-C, Suzuki-Hatano S, Pacak CA. Viral vectors for gene therapy. Molecular Medical Microbiology: Elsevier; 2024. p. 2659-79. doi:10.1016/B978-0-12-818619-0.00019-8.

10. Li X, Le Y, Zhang Z, Nian X, Liu B, Yang X. Viral vector-based gene therapy. *Int J Mol Sci* 2023;24(9):7736. doi:10.3390/ijms24097736

11. Pan X, Veroniaina H, Su N, Sha K, Jiang F, Wu Z, et al. Applications and developments of gene therapy drug delivery systems for genetic diseases. *Asian J Pharm Sci* 2021;16(6):687-703. doi:10.1016/j.ajps.2021.05.003

12. Sahu T, Ratre YK, Chauhan S, Bhaskar L, Nair MP, Verma HK. Nanotechnology based drug delivery system: Current strategies and emerging therapeutic potential for medical science. *J Drug Deliv Sci Technol* 2021;63:102487. doi:10.1016/j.jddst.2021.102487

13. Butt MH, Zaman M, Ahmad A, Khan R, Mallhi TH, Hasan MM, et al. Appraisal for the potential of viral and nonviral vectors in gene therapy: A review. *Genes* 2022;13(8):1370. doi:10.3390/genes13081370

14. Seppala J, Van Bochove B, Lendlein A. Developing advanced functional polymers for biomedical applications. ACS Publications *Biomacromolecules*; 2020. p. 273-5. doi:10.1021/acs.biomac.9b01701

15. Wang C, Pan C, Yong H, Wang F, Bo T, Zhao Y, et al. Emerging non-viral vectors for gene delivery. *J Nanobiotechnology* 2023;21(1):272. doi:10.1186/s12951-023-02044-5

16. Mindemark J, Tabata Y, Bowden T. Low charge density cationic polymers for gene delivery: exploring the influence of structural elements on in vitro transfection. *Macromol Biosci* 2012;12(6):840-8. doi:10.1002/mabi.201100480

17. Sung YK, Kim S. Recent advances in the development of gene delivery systems. *Biomater Res* 2019;23(1):8. doi:10.1186/s40824-019-0156-z

18. Zhao W, Hou X, Vick OG, Dong Y. RNA delivery biomaterials for the treatment of genetic and rare diseases. *Biomaterials* 2019;217:119291. doi:10.1016/j.biomaterials.2019.119291

19. Alhakamy NA, Curiel DT, Berkland CJ. The era of gene therapy: From preclinical development to clinical application. *Drug Discov Today* 2021;26(7):1602-19. doi:10.1016/j.drudis.2021.03.021

20. Nayerossadat N, Maedeh T, Ali PA. Viral and nonviral delivery systems for gene delivery. *Adv Biomed Res* 2012;1(1):27. doi:10.4103/2277-9175.98152

21. Enayati M, Liu W, Madry H, Neisiany RE, Cucchiarini M. Functionalized hydrogels as smart gene delivery systems to treat musculoskeletal disorders. *Adv Colloid Interface Sci* 2024:103232. doi:10.1016/j.cis.2024.103232

22. Paunovska K, Loughrey D, Dahlman JE. Drug delivery systems for RNA therapeutics. *Nat Rev Genet* 2022;23(5):265-80. doi:10.1038/s41576-021-00439-4

23. Kotterman MA, Chalberg TW, Schaffer DV. Viral vectors for gene therapy: translational and clinical outlook. *Annu Rev Biomed Eng* 2015;17(1):63-89. doi:10.1146/annurev-bioeng-071813-104938

24. Ramamoorth M, Narvekar A. Non viral vectors in gene therapy-an overview. *J Clin Diagn Res* 2015;9(1):GE01. 10.7860/JCDR/2015/10443.5394

25. Zu H, Gao D. Non-viral vectors in gene therapy: recent development, challenges, and prospects. *AAPS J* 2021;23(4):78. doi:10.1208/s12248-021-00608-7

26. Van Bruggen C, Hexum JK, Tan Z, Dalal RJ, Reineke TM. Nonviral gene delivery with cationic glycopolymers. *Acc Chem Res* 2019;52(5):1347-58. doi:10.1021/acs.accounts.8b00665

27. Mai K, Zhang S, Liang B, Gao C, Du W, Zhang L-M. Water soluble cationic dextran derivatives containing poly (amidoamine) dendrons for efficient gene delivery. *Carbohydr Polym* 2015;123:237-45. doi:10.1016/j.carbpol.2015.01.042

28. Liang X, Ren X, Liu Z, Liu Y, Wang J, Wang J, et al. An efficient nonviral gene-delivery vector based on hyperbranched cationic glycogen derivatives. doi:*Int J Nanomedicine* 2014:419-35. 10.2147/IJN.S51919

29. Saranya N, Moorthi A, Saravanan S, Devi MP, Selvamurugan N. Chitosan and its derivatives for gene delivery. *Int J Biol Macromol* 2011;48(2):234-8. doi:10.1016/j.ijbiomac.2010.11.013

30. Huang S, Huang G. The dextrans as vehicles for gene and drug delivery. doi:*Future Med Chem* 2019;11(13):1659-67. doi:10.4155/fmc-2018-0586

31. Healy L, Ruban L. Atlas of Human Pluripotent Stem Cells in Culture. New York: Springer; 2015. p. 3-18.

32. Li X, Li N, Wang Y, Han Q, Sun B. Research progress of fibroblasts in human diseases. *Biomolecules* 2024;14(11):1478. doi:10.3390/biom14111478

33. He Y, Han Z, Zhang Q, Liu L, Chang J. Role of fibroblasts in nonfibrotic autoimmune skin diseases. *Mol Med* 2024;30(1):178. doi:10.1186/s10020-024-00949-x

34. Shi Z, Liu Z, Wei Y, Zhang R, Deng Y, Li D. The role of dermal fibroblasts in autoimmune skin diseases. *Front Immunol* 2024;15:1379490. doi:10.3389/fimmu.2024.1379490

35. Xiao X, Chen H, Paerhati P, Zhou M, Yang Z, Bai S, et al. Establishment and Application of Engineered NIH 3T3 Cell Line with Stable Human RAGE Expression. *Pharm Fronts* 2020;2(01):e23-e7. doi:10.1055/s-0040-1708511

36. Leibiger C, Kosyakova N, Mkrtchyan H, Glei M, Trifonov V, Liehr T. First molecular cytogenetic high resolution characterization of the NIH 3T3 cell line by murine multicolor banding. *J Histochem Cytochem* 2013;61(4):306-12. doi:10.1369/0022155413476868

37. Steele TWJ. Oligo-l-lysine-, dextran-, and alkyl-derivatives of polyethylenimine for the development of novel gene transfection vectors: University of Minnesota Minneapolis; 2006.

38. Abdullah S, Wendy-Yeo WY, Hosseinkhani H, Hosseinkhani M, Masrawa E, Ramasamy R, et al. Gene transfer into the lung by nanoparticle dextran-spermine/plasmid DNA complexes. *Biomed Res Int* 2010;2010(1):284840. doi:10.1155/2010/284840

39. Huang G, Huang H. Application of dextran as nanoscale drug carriers. *Nanomedicine* 2018;13(24):3149-58. doi:10.2217/nnm-2018-0331

40. Varshosaz J. Dextran conjugates in drug delivery. *Expert Opin Drug Deliv* 2012;9(5):509-23. doi:10.1517/17425247.2012.673580

41. Maia J, Evangelista MB, Gil H, Ferreira L. Dextran-based materials for biomedical applications. In: Gil MH, editor. Carbohydrates Applications in Medicine. Kerala: Research Signpost; 2014. P. 31-53.

42. Mazumder MAJ, Zahir MH, Zaman SF. Advanced materials for gene delivery. *Adv Mat Res* 2014;995:29-47. doi:10.4028/www.scientific.net/amr.995.29

43. Cai X, Dou R, Guo C, Tang J, Li X, Chen J, et al. Cationic polymers as transfection reagents for nucleic acid delivery. *Pharmaceutics* 2023;15(5):1502. doi:10.3390/pharmaceutics15051502

44. Liu L, Yang Y-L, Wang C, Yao Y, Ma Y-Z, Hou S, et al. Polymeric effects on DNA condensation by cationic polymers observed by atomic force microscopy. *Colloids Surf B Biointerfaces* 2010;75(1):230-8. doi:10.1016/j.colsurfb.2009.08.040

45. Cook AB, Gonzalez BD, van Hest JC. Tuning of Cationic Polymer Functionality in Complex Coacervate Artificial cells for optimized enzyme activity. *Biomacromolecules* 2023;25(1):425-35. doi:10.1021/acs.biomac.3c01063